Determination of the cross section of ^{39}K(n, p)^{39}Ar reaction induced by D-D neutrons with neutron activation and noble gas mass spectrometry techniques*

Xiao-Han Liu (刘笑函)[1,2] Chang-Lin Lan (兰长林)[2†] Hao-Nan Li (李昊南)[2] Bo Gao (高波)[2] Kuo-Zhi Xu (徐阔之)[2]
Jiang-Long Pan (潘江龙)[2] Xiao-Dong Pan (潘小东)[2] Wan-Feng Shi (史万峰)[2] Bao-Chun Li (李保春)[1]
Fei Su (苏菲)[3‡] Huai-Yu He (贺怀宇)[3] Jun-Jie Li (李军杰)[4]

[1]College of Physics and Electronic Engineering, Shanxi University, Taiyuan 030006, China
[2]School of Nuclear Science and Technology, Lanzhou University, Lanzhou 730000, China
[3]The Institute of Geology and Geophysics, Chinese Academy of Geological Sciences, Beijing 100029, China
[4]Beijing Research Institute of Uranium Geology, Beijing 100029, China

Abstract: The cross-sections of ^{39}K(n, p)^{39}Ar at the 2-3 MeV energy play an important role in nuclear structure research and ^{40}Ar/^{39}Ar geochronology application. Due to the limitations of n-^{3}He coincidence technology and counting instruments, the published data from the literature are before 1967, and the existing data are scarce and of significant divergence. Meanwhile, there are large discrepancies between the measured and evaluation results. By taking advantage of the high sensitivity and resolution noble gas mass spectrometer at Institute of Geology and Geophysics, Chinese Academy of Sciences (IGGCAS), the cross-section of ^{39}K(n, p)^{39}Ar were measured by the methods of combined neutron activity analysis and noble gas mass spectrometry techniques, and the uncertainties were discussed in detail. The cross-section of ^{39}K(n, p)^{39}Ar were measured as 103.84 ± 16.33, 109.76 ± 15.88, 150.27 ± 24.19 mb, at 2.56 ± 0.08, 2.69 ± 0.08, 2.96 ± 0.12 MeV energies respectively. The measured data filled the data gaps and provided more accurate data support for ^{40}Ar/^{39}Ar dating. Furthermore the theoretical excitation function of ^{39}K(n, p)^{39}Ar was calculated using TALYS-1.97 computer codes. Then the experimentally determined cross-sections were analyzed by comparing with literature data available in EXFOR database and evaluated nuclear data in ENDF/B-VIII.0, JEFF-3.2, TENDL-2021, BROND-3.1, and JENDL-5 databases. According to comparative results, the measured cross-sections of ^{39}K(n, p)^{39}Ar exhibit a rapid energy-dependent increase between 2-3 MeV, aligning with higher literature values and resolving previous discrepancies. Compared with the previously reported data, the precision of determined cross-sections in this work have great improvement. The comparison of measured data indicates that the combined detection method of neutron activity analysis and noble gas mass spectrometry techniques is suitable for measuring cross-sections of long-life product nuclei nuclear reaction and the application of ^{40}Ar/^{39}Ar geochronology with D-D neutron source.

Keywords: ^{39}K(n, p)^{39}Ar, cross-section, neutron activation, noble gas spectrometer

DOI: **CSTR:**

I. INTRODUCTION

Nuclear data play an important role in applied physics and nuclear physics research, besides the neutron cross-sections are of great significance to fusion reactor [1] and nuclear structures of nuclear reaction [2]. Moreover the cross-section of reaction ^{39}K(n, p)^{39}Ar is of significant importance to the study of the application of ^{40}Ar/^{39}Ar dating technology. There are only three literature contain three data points of the cross-sections of ^{39}K(n, p)^{39}Ar at around 2.5 MeV. The cross-sections of ^{39}K(n, p)^{39}Ar induced by neutron with energy of 2.59 MeV was measured using D-D reactor and n-^{3}He coincidence system by G. Lindström [3] in 1958 for the study of ^{39}Ar nuclear structure. The experimentally obtained cross-sections of ^{39}K(n, p)^{39}Ar was 45 mb with 10% uncertainty. There was an approximately 100% deviation from the 96 ± 6 mb measured by W. R. Dixon [4] in 1961 at 2.49 MeV. Although the results exhibit a law of rapid energy-dependent increase between 2-3 MeV energy in the

Received 10 July 2025; Accepted 19 December 2025
* Supported by the National Nuclear Energy Development Project (HNKF202327 (36)), and the National Natural Science Foundation of China (41573050).
† E-mail: lanchl@lzu.edu.cn
‡ E-mail: sufei@mail.iggcas.ac.cn

R. Bass [5] research, the nearly 100% deviation is obviously abnormal. P. B. Johnson replicated the experiment of Dixon in 1967 and acquired the cross-sections data was 95 ± 4 mb at neutron energy of 2.46 MeV [6]. ^{3}He long counter and KI(Tl) detector were used in n-^{3}He coincidence system for the counts of emitted ^{3}He and the ^{39}K neutron induced reactions respectively. The ^{3}He long counter has to resolve the protons, tritons and ^{3}He recoil particles signal of the D(d, p)T and D(d, n)^{3}He reaction from the D-D reaction. Despite considerable efforts to mitigate the influence of charged particles other than ^{3}He, the outcomes have been suboptimal. Existing methods either inadequately shield non-target charged particles or only partially attenuate non-^{3}He charged particles [7-9], thereby compromising the accuracy of the data.

The cross-sections of ^{39}K(n, p)^{39}Ar are also of great significance to improved ^{40}Ar/^{39}Ar geochronology. ^{40}Ar/^{39}Ar dating is one of the most widely applied geochronological methods in Earth sciences [10]. A key step in this method involves converting ^{39}K to ^{39}Ar via neutron irradiation. The ^{40}Ar/^{39}Ar age is calculated using the following equation:

$$t = \frac{1}{\lambda}\ln\left(1 + \frac{^{40}Ar^{*}}{^{39}Ar} \times J\right) \tag{1}$$

J in Eq. (1) is

$$J = \frac{\lambda}{\lambda_e} \times \frac{\int \Phi(E) \times \sigma(E) \mathrm{d}E}{^{40}K/^{39}K} \tag{2}$$

Where the E represents the energy of neutron irradiation, the $\Phi(E)$, $\sigma(E)$ represent the neutron fluence and the cross section of ^{39}K(n, p)^{39}Ar at neutron reaction energy E respectively, ^{40}K, ^{39}K is the potassium isotope ^{40}K, ^{39}K content of dating samples, $^{40}Ar^{*}$ is the radiogenic ^{40}Ar from ^{40}K decay, ^{39}Ar is the content of ^{39}Ar from the neutron reaction ^{39}K(n, p)^{39}Ar, λ is the total decay constant of ^{40}K, and λ_e is the electron capture decay constant of ^{40}K.

Typically, J value is determined using samples of known age as neutron flux monitors. Renne et al. [11] proposed the use of D-D neutron sources in ^{40}Ar/^{39}Ar dating. Owing to the excellent mono-energetic neutron of D-D neutrons, the Eq. (2) can be reformulated to $J = \frac{\lambda}{\lambda_e} \times \frac{\Phi \times \sigma}{^{40}K/^{39}K}$, the neutron fluence and cross-section can be directly determined by the irradiation experimental sample to get J-value directly. The D-D neutron source mitigates issues such as the interference reactions and nuclear recoil associated the broad energy spectrum of the conventional reactor-based neutron sources [12-14]. The cross-sections of ^{39}K(n, p) reaction in 2-3 MeV neutron energy range are crucial for absolute ^{40}Ar/^{39}Ar dating, as this energy range corresponds to typical D-D neutron energies and exhibits a rapid increase in cross-section. However, only three data points are available around 2.5 MeV. The evaluated data of ^{39}K(n, p)^{39}Ar cross-sections in ENDF/B-VIII.0 differ from the existing experimental values by over 90%. Moreover, cross-sections values from different nuclear data libraries show substantial discrepancies near 2.5 MeV. The cross-sections of ^{39}K(n, p)^{39}Ar near 2.5 MeV from ENDF/B-VIII.0, JEFF-3.3, TENDL-2021, BROND-3.1, JENDL-5, and relevant published literature are summarized in Table 1 [15-19].

In the 2-3 MeV energy range, there have been no attempts to remeasure the cross-sections of ^{39}K(n, p)^{39}Ar since 1967. Moreover, n-^{3}He coincidence technique has problems of long counter count inaccurate caused by scattered particles at large angles and non-^{3}He signal peak overlap, which directly affect the accuracy of coincidence counts and ^{3}He total counts. As a result, the experimental cross-sections data of ^{39}K(n, p)^{39}Ar around 2.5 MeV are only three data points, the available data differ widely, the precision of the experimental data is low and the development of absolute ^{40}Ar/^{39}Ar dating method was limited by poor reliability and accuracy data. Considering the divergence and scarcity of ^{39}K(n, p) cross-sections in 2-3 MeV energy and the poor accuracy, it is necessary to remeasure the cross section to fill the data gaps and provide reliable data for requirements of modern experiments.

With the development of noble gas mass spectrometry technology, argon can be accurately measured. We have proposed a detection method that combines neutron activation and mass spectrometry to conduct high-precision cross-sections measurements of ^{39}K(n,p)^{39}Ar instead of detecting the n-^{3}He coincidence signal. The combined method above avoids the problems of large-angle particles scattering and ^{3}He spectral overlap of n-^{3}He coincidence system. Neutron activation analysis (NAA) is a highly mature technique used for neutron reaction energy and flux in the detection of cross-sections [20, 21]. As a most sensitive technology for the detection of argon to date, noble gas mass spectrometers have significantly

Table 1. The cross-sections of ^{39}K(n, p)^{39}Ar in 2-3 MeV neutron energy from available published literature and nuclear databases.

NeutronEnergy(MeV)	Cross-section(mb)	Reference
2.59	45 with 10%	Lindström [3]
2.49	96 ± 6	Dixon [4]
2.46	95 ± 4	Johnson [6]
2.50	187.86	ENDF/B-VIII.0 [15]
2.50	163.24	JEFF-3.3 [16]
2.50	166.04	TENDL-2021 [17]
2.50	118.25	BROND-3.1 [18]
2.50	116.28	JENDL-5 [19]

high resolution and low-concentration detection capability of Ar isotope. With the multi-collector and CFM [22, 23] (combined Faraday counting CDD (Compact Discrete Dynote) multiplier), noble gas mass spectrometers have good precision of different mass argon isotopes (^{36}Ar, ^{37}Ar, ^{39}Ar, ^{40}Ar) and weak signal as ^{39}Ar, which is suitable for detection of argon.

In present work, a detection method for cross-sections of ^{39}K(n, p)^{39}Ar based on the combination of neutron activation analysis (NAA) and noble gas mass spectrometer (NGMS) technique was established. The neutron flux can be obtained using the γ-ray spectrum of activity monitor in neutron activation technique, and the number of reaction nucleus ^{39}Ar can be obtained by noble gas mass spectrometry technique. The cross-sections of ^{39}K(n, p)^{39}Ar were determined at 2.56 MeV, 2.69 MeV, 2.96 MeV mean neutron energy using high sensitivity and high-resolution instrument. The reliability and precision of measured cross-sections was discussed by compared with previous literature data, evaluated data of databases and TALYS-1.97 theoretical calculation data.

II. EXPERIMENT

A. Theoretical formula

The cross-sections of ^{39}K(n, p)^{39}Ar was determined by measuring the full-energy peak of monitor (^{58}Ni) characteristic γ-ray and the ^{39}Ar content of activated sample. The potassium samples sandwiched with the nickel monitors were irradiated by neutron emitted from D(d, n)^{3}He. The gamma spectrum of activated nickel samples was obtained by off-line γ-ray spectrometric technique with high resolution and low background HPGe detector for the determination of neutron fluence. Then the ^{39}Ar content of irradiated samples was measured by noble gas mass spectrometer. According to the definition of cross-sections, the measurement equation is followed,

$$\sigma = \frac{N_{\mathrm{Ar}}}{N_{\mathrm{K}}\Phi} \tag{3}$$

$\Phi = \varphi$T total neutron fluence; φ neutron flux; T total irradiation time; N_{Ar} the mole of ^{39}Ar from ^{39}K(n, p) reaction; N_{K} the mole of ^{39}K from target sample; The N_{Ar} representing the number of nuclear reactions.

B. Neutron source

The irradiation was carried out using the CPNG-600 neutron generator at China Institute of Atomic Energy (CIAE). The time of lasted irradiation was approximately 94.5 h. The neutrons were produced by D(d, n)^{3}He reaction with a deuteron ion (D^+) beam current of 300 μA, and the energy of deuteron ion beam was 300 keV approximately. The thickness of solid deuterium-titanium target used in generator was approximately 1mg/cm^2. The yield of CPNG-600 is approximately 7.5×10^8 n/s. An Au-Si surface barrier detector was installed at 135° respect to the D+ beam. The associated protons of D(d, p)T reaction, representing the neutron of D(d, n)^{3}He, were recorded every three hundreds seconds to determine the neutron fluency fluctuation.

C. Samples irradiation and neutron energy determination

Potassium-bearing samples SK01 sanidine, containing 8.62% potassium, were provided by IGGCAS [24]. The selected SK01 sanidine samples are standard materials used in ^{40}Ar/^{39}Ar geochronology and widely applied in age determination. The detail parameters of samples are shown in Table 2. The information of main reaction ^{39}K(n,p)^{39}Ar is shown in Table 4. Three samples were packed into circular discs of 20 mm diameter. Each labeled sample was sandwiched between two nickel foils (99.99% purity, 0.5 mm thick each foil) of the same diameter, which served as neutron flux monitors. The assembled Ni–SK01–Ni structures were wrapped with plastic film. The wrapped samples were placed at 0°,45°,90° relative to the D^+ beam direction and center of the D-Ti target at a distance of approximately 4 cm. The placement diagram of sandwiched samples are shown in Fig. 1.

The neutron mean energy emitted at angle β was determined by cross-sectional ratio method of reactions ^{64}Zn(n, p)^{64}Cu, ^{115}In(n, n')$^{115\ m}$In [25, 26] and checked with the Eq. (4) based on Q equation from J.H. Luo [27]. The mean neutron energy calculated geometric model is shown in Fig. 2.

$$\overline{E} = \frac{2L}{\pi R^2}\int_{\beta-\arctan(\frac{R}{L})}^{\beta+\arctan(\frac{R}{L})} E_n(\theta, E_d)\frac{\sqrt{R^2 - L^2\tan^2(\beta-\theta)}}{\cos^2(\beta-\theta)}\mathrm{d}\theta \tag{4}$$

Q equation is as followed,

$$E_n(\beta, E_d) = \left\{\frac{\sqrt{2E_d}}{4}\cos(\beta) + \left[\left(\frac{1}{2} + \frac{1}{8}\cos^2(\beta)\right)E_d + \frac{3}{4}\mathrm{Q}\right]^{\frac{1}{2}}\right\}^2 \tag{5}$$

Table 2. Samples information

Sample	Number	Diameter of Samples (mm)	Mass of Samples (mg)
SK01	1#	20	204.9
	2#	20	204.1
	3#	20	209.5

The nickel samples were also cut into discs with a diameter of 20mm.

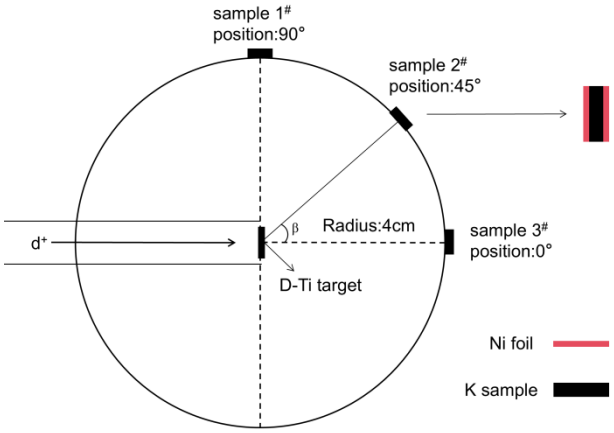

Fig. 1. (color online) The geometric model of sample and d-d generater.

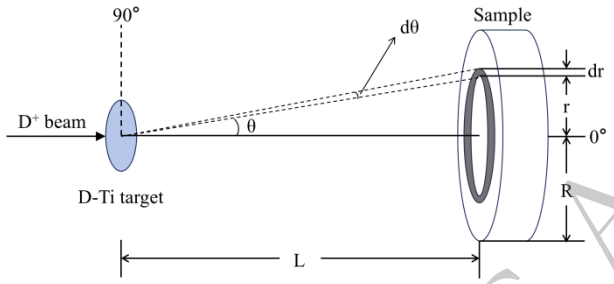

Fig. 2. (color online) The schematic diagram of mean energy calculated geometric model.

The β is the angle between the d^+ beam direction and the line from D-Ti center to sample center. The mean neutron energy at samples 1, 2, 3 were calculated as 2.56±0.08 MeV, 2.69±0.08 MeV, 2.96±0.12 MeV respectively.

D. The measurement of neutron flux by ^{58}Ni activity

^{58}Ni and ^{54}Fe isotopes are found to be the suitable neutron flux monitors as the cross-sections of ^{58}Ni(n, p)^{58}Co and ^{54}Fe(n, p)^{54}Mn are similar to that of ^{39}K(n, p)^{39}Ar at 2-3 MeV (The cross-sections of these reactions are shown in Fig. 3). The neutron flux detected by the similar cross-section is closer to the actual neutron flux when the sample was irradiated. The isotopic abundance of ^{54}Fe is only 5.845%, while that of ^{58}Ni is 68.077%, and the characteristic gamma-ray intensities of products ^{58}Co and ^{54}Mn are similar. Under the same mass and irradiation conditions, a large number of radioactive product nuclei can be generated from nickel foil, and more γ-ray full-energy peak signal will be detected, reducing the statistical error. If ^{54}Fe is enriched, the preparation would be difficult and the cost would be high. Considering the simplicity and cost of the experiment, ^{58}Ni and ^{58}Ni(n, p)^{58}Co were chosen as the isotope and reaction to monitor neutron flux. The neutron flux were determined by gamma spectrum of activated nickel samples, using low background γ-ray spectrometer equipped with high resolution HPGe detector. The decay γ-ray was emitted by ^{58}Co from the activation reaction ^{58}Ni(n, p)^{58}Co of nickel samples.

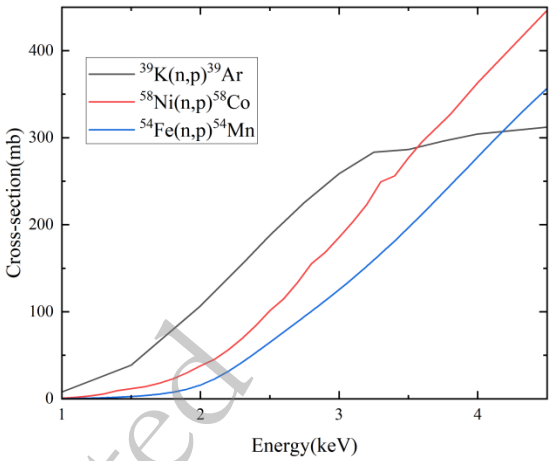

Fig. 3. (color online) The Cross-sections of ^{39}K(n, p)^{39}Ar, ^{58}Ni(n, p)^{58}Co, and ^{54}Fe(n,p)^{54}Mn at neutron energy of 1-4.5 MeV.

The GEM60P type HPGe detector (provided by Department of Nuclear Physics, CIAE) has a relative efficiency of 68% and a resolution of 1.82 keV at 1.33 MeV energy. The ^{58}Ni was chosen for the activity detection of neutron flux, because the cross-sections excitation function of ^{58}Ni(n, p)^{58}Co is similar to ^{39}K(n, p)^{39}Ar at the 2-3 MeV energy, which reducing system errors. The activated nickel samples were placed 15 cm away from the detector, the dead time is less than 0.5% and the decay γ-ray spectrum of neutron activation product ^{58}Co was detected and unfolded by energy spectrum analysis software MAESTRO from ORTEC (company in USA).

Neutron activation analysis time was divided into 3 parts as T_1, T_2, T_3. T_1 is the irradiation time , T_2 is the cooling time from the end of irradiation to the start of gamma spectrum detection, T_3 is the measurement time of gamma spectrum detection. According to the parameters of monitor and the full-energy peak γ-ray spectrum diagram from off-line γ-ray spectrometry, the equation for neutron activation analysis is as follows,

$$FC = \frac{KMN_A\eta\varphi\sigma I_\gamma\varepsilon^p}{\lambda A} S D \tag{6}$$

the neutron flux are calculated by Eq. (7)

$$\varphi = \frac{FC\lambda A}{KMN_A\eta\sigma I_\gamma\varepsilon^p S D} \tag{7}$$

For a reaction of X(n, b)Y, where M is mass of the sample, A is atomic weight of the parent nucleus, η is the abundance of X, σ is the cross-sections of X(n, b)Y, φ is

the mean neutron flux, I_γ is decay γ-ray intensity of activated monitor ^{58}Co , λ is decay constant, N_A is Avogadro constant, ε^p is full-energy peak efficiency, C is the total counts in the γ-ray full-energy peak. $S=(1-e^{-\lambda T_1})$ is growth factor, $D=e^{-\lambda T_2}(1-e^{-\lambda T_3})$ is counting collection factor.

F is total correction factor of the activity, $F=F_s\times F_c\times F_g$, Fs, Fc, Fg are γ-ray self-absorption, γ-ray coincidence summing effects and sample geometry factor respectively.

K is neutron fluency fluctuation factor [28],

$$K=[\sum_{i}^{L}\varphi_i(1-e^{-\lambda\Delta t_i})e^{-\lambda T_i}]/\varphi S \tag{8}$$

In this work, we divided total irradiation time into L part, where L is the number of time intervals into which the irradiation time is divided. Δt_i is the duration of the ith time interval, T_i is the time interval from the end of the ith interval to the end of irradiation, φ_i is the neutron flux averaged over the sample during the Δt_i, φ is the neutron flux averaged over the sample during the total irradiation time T. Long time neutron irradiation as 94.5h may cause neutron flux fluctuation, therefore we calculated K factor by detecting the associated proton particles which represents the neutron flux in L parts of time to fix results. The recorded time Δt_i was set 300 second in each part of L parts.

The measurement neutron flux differences caused by the self-absorption effect were taken into account. The first to consider was the self-absorption effect of gamma rays. The formula of self-absorption coefficient F_s is shown in below,

$$F_s=\frac{1-e^{-\mu(E)x}}{\mu(E)x} \tag{9}$$

$\mu(E)$ is the energy-dependent mass attenuation coefficient ($cm^2\cdot g^{-1}$), E=810.67 keV.

x is the mass thickness, $x=\rho d$, ρ is the density of nickel, d is the thickness of Ni sheet.

Secondly, there is the neutrons attenuation in SK01 sample, which is neutron self-absorption. We separately calculated the neutron flux of two sandwiched Ni sheet in each samples. According to neutron attenuation effect, the average neutron flux of sample is calculated by Eq. (10).

$$\overline{\varphi}=\varphi_1\left(\frac{1-e^{-\omega s}}{\omega s}\right) \tag{10}$$

Where the $\overline{\varphi}$ is the average neutron flux of sample, φ_1 is the neutron flux determined by Ni which is close to the D-Ti target, ω is the linear attenuation coefficient, $s=h_2$-h_1, h_1 is the distance between the center of D-Ti target and Ni sheet close to D-Ti target, h_2 is the distance between the center of D-Ti target and Ni sheet far away from D-Ti target,

In this work the linear attenuation coefficient was determined by Eq. (11)

$$\varphi_2=\varphi_1\frac{h_1^2}{h_2^2}e^{-\omega s} \tag{11}$$

Where φ_2 is the neutron flux determined by Ni which is far away from the D-Ti target,Part of self-absorption parameters of Sample 3$^{\#}$ are shown in Table 3.

Table 3. The self-absorption parameters of Sample 3$^{\#}$

Parameter symbol	value
$\mu(E)$	6.846×10^{-2} cm^2/g
x	0.445 g/cm
h_2	5.25 mm
h_1	4.25 mm
s	1 mm
ω	0.803 cm^{-1}

The gamma self-absorption factor F_s = 1.0153, which results in an increase of about 1.5% in the calculated neutron flux. Taking into account the neutron self-absorption effect, compared with not considering that, the neutron flux of sample 3$^{\#}$ decreases approximately 4% and the neutron flux of samples 1$^{\#}$ and 2$^{\#}$ decease less than 1%. Overall, the impact of self-absorption on the final measured cross-section is approximately 2.5% for sample 3$^{\#}$, and less than 1% for samples 1$^{\#}$ and 2$^{\#}$.

The detection efficiency ε^p was determined by the well-known standard source ^{152}Eu placing 15 cm at HP-Ge detector, using Eq. (12).

$$\varepsilon^p=\frac{C'}{A_0 I_\gamma t\exp(-\lambda T)} \tag{12}$$

Where the C' is the nut count of ^{152}Eu full energy peak in the counting time t, A_0 is the source activity at time of manufacturing, T is the time from the data of manufacturing to the start time of detection, λ is the decay constant of standard source, and the I_γ is the intensity of characteristic γ-ray.

The detection efficiency was obtained by γ-ray full-energy counts of standard source ^{152}Eu. The half-life and radioactive activity at the manufacturing time of the standard source ^{152}Eu were 13.517 a and 132192 Bq respectively. There is a linear relationship between energy and ε under the exponential form. The fitting formula is as follows,

$$ln(\varepsilon) = \sum_{j=1}^{n} a_j (ln(E/E_0))^{j-1} \quad (13)$$

Where the a_j is the fitting parameter, the goodness of fit value is observed for j=3 with $\frac{\chi_j^2}{(11-3)} \approx 1$ [29]. May as well set $E_0 = 1$ keV , the polynomial function is given as,

$$ln(\varepsilon) = -3.3454 + 0.03015 * ln(E) - 0.06037 * (ln(E))^2 \quad (14)$$

The R square is 0.997.

The σ in Eq. (7) is the standard cross-section of ^{58}Ni(n, p)^{58}Co determined by the mean energy which is calculated in Eq. (4). The cross-sections of activation reaction ^{58}Ni(n, p)^{58}Co were 109.38±12.18 mb, 131.76±16.12 mb, 178.65±19.80 mb relative to the calculated neutron mean energy 2.56±0.08 MeV, 2.69±0.08 MeV, 2.96±0.12 MeV respectively getting from ENDF/B-VIII.0 [15] database.

The measured ^{58}Co γ-ray spectrum is shown in Fig. 4. The constants of Ni samples are shown in Table 4. From the above measured data, we brought it into Eq. (7) to calculate the mean neutron flux.

E. ^{39}Ar content detection using noble gas mass spectrometry

Ar isotopic analyses were carried out in noble gas laboratory, at Institute of Geology and Geophysics, Chinese Academy of Sciences (IGGCAS, Fig. 5). Samples were step-heated from 970 ℃ to 1300 ℃ in 10–50 ℃ increments to release the gases. During each step noble gases, H_2O, CO_2, and various hydrocarbons were released concurrently. Liquid-nitrogen traps removed H_2O and CO_2, and GP50 SAES getters further stripped hydrocarbons before the purified gas entered the mass spectrometer. However, residual hydrocarbons still influenced the low-abundance isotope ^{39}Ar. Argon isotopes were measured with a Noblesse multi-collector mass spectrometer. The instrument is equipped with a Nier-type ion source, a 240 mm radius magnet, one Faraday cup, and three electron multipliers. The ^{40}Ar sensitivity of the mass spectrometer is 1.2×10^{-3} A/Torr, with a mass resolution greater than 700. Isotopes were acquired in peak-jump mode. ^{40}Ar was recorded on the Faraday cup, whereas ^{39}Ar, ^{38}Ar, ^{37}Ar, and ^{36}Ar were measured on the multipliers in ion counting mode. Data reduction included blank subtraction, mass-discrimination correction, interference correction, and correction for the ^{40}Ar peak tail. A procedural blank, following the same extraction sequence as the samples, was run before each unknown. The ^{40}Ar blank contribution was <1 %, and the ^{38}Ar , ^{36}Ar blank was <5 % of the respective signals. Air calibrations ("air shots") were used to monitor instrumental mass discrimination. The discrimination factor averaged 0.9985 ± 0.0052. Interferences on ^{39}Ar (e.g., $H_2{}^{37}Cl$, C_3H_3) [30] were minimized by precise peak centering and subsequently corrected (Fig. 6). Because ^{40}Ar is 4–5 orders of magnitude more abundant than ^{39}Ar, the effect of ^{40}Ar tailing on the adjacent ^{39}Ar peak was evaluated. Tests on atmospheric standards devoid of ^{39}Ar showed that ^{40}Ar tailing contributed <0.3 ppm to the apparent ^{39}Ar signal. Corrected ^{39}Ar abundances are reported in Table 5.

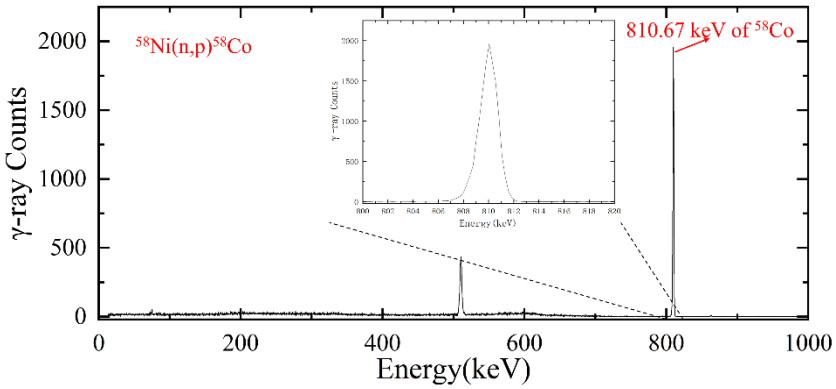

Fig. 4. (color online) The tapical γ-ray spectrum of ^{58}Co measured by off-line γ-ray spectrometer equipped with HPGe detector.

Table 4. The main reaction data of irradiated samples

Reaction	Abundance of target isotope η (%)[a]	Half-life of product $T_{1/2}$	γ-ray energy E_γ (keV)[b]	γ-ray intensity I_γ (%)[c]
^{58}Ni(n,p)^{58}Co	68.007	70.860d	810.759	99.45
^{39}K(n,p)^{39}Ar	93.258	268y	-	-

a. The abundance of target isotope represents ^{58}Ni and ^{39}K isoptopes of natual elements in samples respectively. b. The half-lives of products represents the half-lives of ^{58}Co and ^{39}Ar in irradiated samples respectively. c. The γ-ray energy and intensity are those of the decay γ-rays of product ^{58}Co.

Fig. 5. (color online) Photo of Noble gas laboratory in IGGCAS.

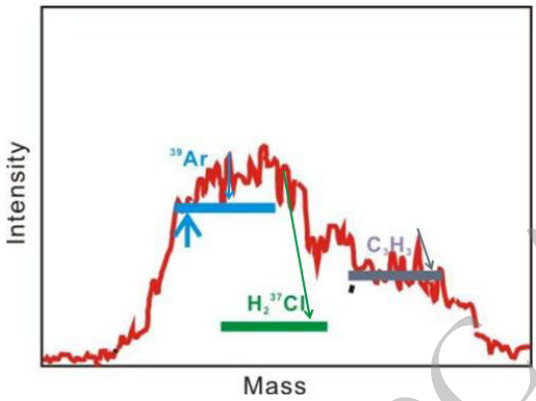

Fig. 6. (color online) Schematic diagram of the peak position of mass number 39, where the blue, green and purple lines are the peak widths of ^{39}Ar, $H_2{}^{37}Cl$, C_3H_3, respectively, and the blue arrows are the measured positions of ^{39}Ar, independent of interference.

III. THEORETICAL CALCULATION OF COMPUTER CODE TALYS

TALYS is a computer program that can analysis the nuclear reactions cross-sections of protons [31], neutrons, photons, deuterons, tritons, ^{3}He and α particles, in the eV-200 MeV energy range and target nuclei masses of 12 or heavier. The cross-sections can be obtained considering optical model for direct reactions, pre-equilibrium reactions and compound reactions in TALYS-1.97. The optical model potentials parameters for neutrons were obtained by local and global parameterizations of Koning and Delaroche [32].The direct reaction contribution was considered and calculated with Distorted Wave Born Approximation DWBA using ECIS-06 code. Two-component exciton model developed by Kalbach [33] was used for calculating pre-equilibrium reaction contribution. And the compound reaction contribution was processed using Hauser-Feshbach statistic model with width fluctuation of Moldauer expression model [34, 35]. The default values were used for parameters concerning nuclear masses, discrete levels, pre-equilibrium and photon strength functions in TALYS calculation, and the level densities and optical model were adjusted (ldmodel 2, rvadjust n 1.16, avadjust n 1.04, rwdadjust n 0.98, awdadjust n 0.98). The theoretical data achieved a high consistency with the evaluated data at low and high energy region and achieved a high consistency with the experimental data at medium energy region (4-9 MeV). Meanwhile the all other out going channels were considered include (n, α) induced reactions and inelastic scattering. The cross-sections of ^{39}K(n, p)^{39}Ar were simulated by TALYS-1.97 with the energy reaching up to 20 MeV.

Table 5. The measured ^{39}Ar content of samples

Sample No.	^{39}Ar content (mol)
1#	$(6.96\pm0.44)\times10^{-17}$
2#	$(1.11\pm0.06)\times10^{-16}$
3#	$(4.58\pm0.29)\times10^{-16}$

IV. RESULTS AND DISCUSSION

A. Results

The cross-sections of the ^{39}K(n, p)^{39}Ar were determined by the measured content of ^{39}Ar and the characteristic γ-ray full-peak counts of activated monitor γ-ray spectrum. The mean neutron energy, total neutron fluence $\Phi_{tot,}$ ^{39}Ar content and ^{39}K(n, p) reaction cross-sections values measured for each sample are summarized in Table 6 according to the sample number. The cross-sections of samples are 103.84±16.33 mb, 109.76±15.88 mb, 150.27±24.19 mb at mean neutron energies 2.56±0.08 MeV, 2.69±0.08 MeV, 2.96±0.12 MeV respectively. The measured cross-sections in this study are plotted in Fig. 7 and Fig. 8 along with the already existing experimental data reported in EXFOR database. Moreover, the present results are compared with evaluated nuclear data from ENDF/B-VIII.0, JEFF-3.3, TENDL-2021, BROND-3.1 and JENDL-5 databases and the code TALYS-1.97.

B. Uncertainty

The uncertainties of neutron flux are caused by detection efficiency of HPGe detector and the mean neutron energy.

The detection efficiency ε^p is calculated by Eq. (12), according to the polynomial fitting results, the uncertainty of detection efficiency at 810.67 keV is approximately 3%.The monitor reaction cross-sections uncertainty is approximately 5.2%, because of neutron mean energy calculated by the angle β and the diameter of sample. The uncertainty of neutron fluence is calculated approximately 2.5%. The uncertainty of counting statistics is 0.8%. The total correction factor of the activity F are the self-

Table 6. The experimental data of ^{39}K(n, p)^{39}Ar cross-sections

Sample No.	Values and results				
	M (mg)	E_n (MeV)	Φ_{tot} (n/cm^2)	^{39}Ar(mol)	σ_K(mb)
1#	204.9	2.56±0.08	1.48×10^{12}	6.96×10^{-17}	103.84±16.33
2#	204.1	2.69±0.08	2.24×10^{12}	1.11×10^{-16}	109.76±15.88
3#	209.5	2.96±0.12	6.58×10^{12}	4.58×10^{-16}	150.27±24.19

σ_K means the cross-section of ^{39}K(n, p)^{39}Ar.

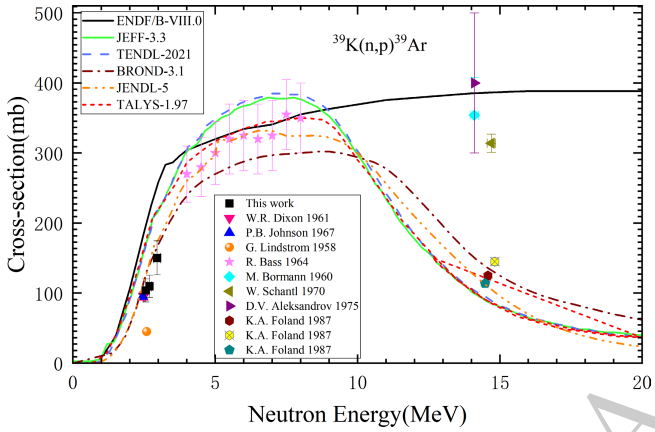

Fig. 7. (color online) The comparing of data include the ENDF/B-VIII.0, JEFF-3.3, TENDL-2021, BROND-3.1, JENDL-5, TALYS-1.9 model code, other's experiment and this work.

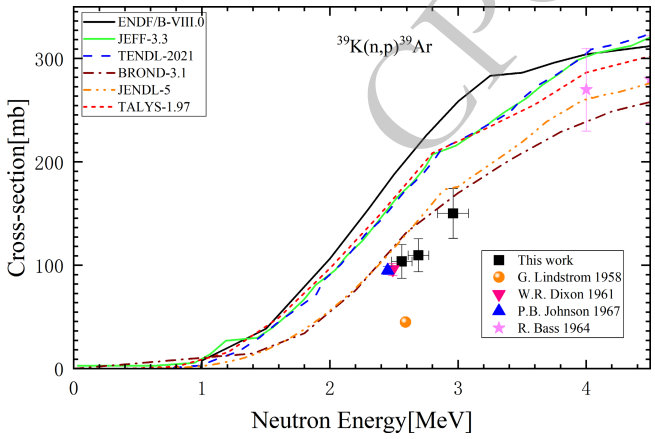

Fig. 8. (color online) The cross-sections of ^{39}K(n, p)^{39}Ar at 0-4.5 MeV mean neutron energy region.

absorption of γ-ray (~1%), the coincidence summing effect of cascade γ-rays (~1%) and the sample geometry (~1%). The weight of samples is less than 0.1%. The neutron fluency fluctuation factor K is approximately 0.1%. The uncertainty of Ar isotopes measurement is approximately 6%, due to the low abundance of mass 39 elements and the uncertainty of the volume of measuring system. The uncertainties have been listed in the Table 7 for reference. The total uncertainty were calculated by quadratic method.

Table 7. Uncertainties of ^{39}K(n,p)^{39}Ar cross-section

Source of Unertainty	Symbol	Estimated Values (%)	Remarks
Counting statistics	C	0.8	Calculated by $1/\sqrt{C}$
Weight of samples	M	<0.1	
Detection efficiency	ε^p	3	
Self-absorption	F_s	1	
Coincidence summing effect	F_c	1	
Sample geometry	F_g	1	
Neutron fluency fluctuation	K	0.1	
Times	T	1.6	Including irradiation(T_1), cooling(T_2), measuring(T_3) times
Cross-section of ^{58}Ni(n, p)^{58}Co	σ_{Ni}	5.2	
Neutron fluence	Φ_{tot}	2.5	
^{39}Ar isotope measurements	^{39}Ar	6	

The detection of argon content contributed most of the uncertainty, mainly because the ^{39}Ar produced by neutron irradiation was insufficient, slightly higher than the background mass of 39. ^{39}Ar yield is determined by irradiation neutron flux and time, the irradiation time took into account the half-life of the activation monitor and the yield of argon. The neutron flux was bound by the neutron source intensity of CPNG-600, which was 7.5×10^8 n/s in this work. The neutron flux generated at the samples was relatively low, and coupled with the time limitation, making the products ^{39}Ar insufficient.

C. Discussion

Compared with the the available literature determined cross-sections and evaluation databases shown in the Fig. 7, the measured data complied with the law that the cross-sections increased rapidly in the energy range of 2-3 MeV. In order to more clearly comparing the measured data with the other researchers and evaluated data, we enlarged the image in the energy range of 1-4.5 MeV, which is shown in Fig. 8. As shown in Fig. 8, In addition, the excitation function calculated by TALYS-1.97 is

shown in Fig. 7 and Fig. 8 which is close to the evaluated data curve of JEFF-3.3 and TENDL-2021. The measured data in this work are close to the data measured by Dixon in 1961, clarifying data deviation between G. Lindström and others. It is highly likely that as P. B. Johnson [6] inferred, in paper of Lindström the (n, α) and (n, p) double peaks are actually a single peak of (n, p). After treating it as a single peak, the cross-section of 81 mb is still much lower than the evaluation value. It can be inferred that the main reason is that deuterium signal and other non-^{3}He signals were confused with the ^{3}He signal, resulting in an overestimation of the ^{3}He reading and ultimately the smaller calculation of cross-sections. measured data in this work are close to evaluated data of JENDL-5 and BROND-3.1 databases. And the JENDL-5 database focuses more on the fitting of experimental data and the evaluation of covariance data [19]. The measured cross-sections are consistent with the physical laws and close to the evaluation excitation function and the previously published experimental data, which shows that our proposed detection method of combined NAA and NGMS techniques to measure the absolute matter content and neutron flux for determination of cross-section is feasible and reliable.

The black filled square are the data determined in this work. The error regarding energy is relatively small and the error bars are covered by the data points. In the following illustration, they have been enlarged for easier reference.

In the enlarged figure, only the data points and legends within the energy range of 0-4.5 MeV are retained, and the retained legends are consistent with Fig. 7.

V. CONCLUSION

In present work, the cross-sections of ^{39}K(n, p)^{39}Ar reaction were determined by the combined detection method of NAA and NGMS techniques. The cross-sections data were obtained by activated sample and monitor of 103.84±16.33, 109.76±15.88, 150.27±24.19 mb at mean neutron energy 2.56±0.08, 2.69±0.08, 2.96±0.12 MeV respectively. Moreover, the excitation function of cross-sections was calculated theoretically by TALYS-1.97 codes. The measured cross-sections of ^{39}K(n, p)^{39}Ar were compared with the evaluation functions of ENDF/B-VIII.0, JEFF-3.3, TENDL-2021, BROND-3.1, JENDL-5 databases, the previously available literature data, and theoretical calculated evaluation function of TALYS-1.97.

Compared with reported literature data in EXFOR database and evaluated data from five databases and the theoretical calculation from TALYS-1.97, the measured cross-sections of ^{39}K(n, p)^{39}Ar in this study are proved to be reliable enough to fill the data gaps of databases. The absolute measurement of ^{39}K, ^{39}Ar content and γ-ray full peak counts with the high sensitivity and resolution instruments in NAA and NGMS combined detection method avoid peak overlap problem, and the precision of the cross-sections of ^{39}K(n, p)^{39}Ar reaction obviously have been improved by high resolution laboratory apparatus.

Although there is still a problem of insufficient argon production, the problem will be gradually solved as the neutron generator yield increases and the resolution of the mass spectrometer improves. It is foreseeable that the method combined with NAA and NGMS will be more accurate in measuring neutron reaction cross-sections in the future. Furthermore the combined method of NAA and NGMS can be applied to the process of ^{40}Ar/^{39}Ar dating to replace nuclear reactor irradiation and improve the problems of Ar nuclear recoil and excessive interference reactions.

ACKNOWLEDGMENTS

The authors are grateful to the staff of the CPNG-600 neutron generator at China institute of atomic energy, for help in the daily maintenance and operation. The authors also thanks to the staff of Noblesse noble gas mass spectrometer at Institute of Geodesy and Geophysics, Chinese Academy of Sciences for help in maintenance.

References

[1] C. Wen, Z. Han, and X. B. Luo, Chin. Phys. C **47**, 024002 (2023)
[2] D. B. Nichols, and M. T. McEllistrem, Phys. Rev. **166**, 1074 (1968)
[3] G. Lindström, and H. Neuert, Z. Naturforsch. A 13: 826-829 (1958)
[4] W. R. Dixon, and J. H. Aitken, Nucl. Phys. 24: 456-464 (1961)
[5] R. Bass, U. Fanger, and F. M. Saleh, Nucl. Phys. 56: 569-576 (1964)
[6] P. B. Johnson, N. G. Chapman, and J. E. Callaghan, Nucl. Phys. A 94: 617-624 (1967)
[7] P. L. Okhuysen, E. W. Bennett, J. B. Ashe *et al.* , Rev. Sci. Instrum. 29: 982-985 (1958)
[8] P. Shapiro, and R. W. Higgs, Phys. Rev. **108**, 760 (1957)
[9] W. Franzen, P. Huber, and L. Schellenberg, Z. Naturforsch. A 10: 820-825 (1955)
[10] S. Kelley, Rev. Mineral. and Geochem. 47: 785-818 (2002)
[11] P. R. Renne, K. B. Knight, S. Nomade *et al.* , Appl. Radiat. Isot. 62: 25-32 (2005)
[12] I. Osborne, S. Sherlock, M. Anand, and T. Argles, Precambrian Res. 189: 91-103 (2011)
[13] D. P. West Jr, and D. R. Lux, Earth Planet. Sci. Lett 120: 221-237 (1993)
[14] S. Kelley, Chem. Geol. 188: 1-22 (2002)
[15] D. A. Brown, M. B. Chadwick, R. Capote *et al.* , Nucl. Data

Sheets 148: 1-142 (2018)
[16] A. J. M. Plompen, O. Cabellos, C. De Saint Jean *et al*., Eur. Phys. J. A **56**, 181 (2020)
[17] A. J. Koning, D. Rochman, J. Sublet, *et al*., Nucl. Data Sheets **155**, 1 (2019)
[18] A. I. Blokhin, E. V. Gai, A. V. Ignatyuk *et al*., Yad. Reak. Konst. No. **2**, 62 (2016)
[19] O. Iwamoto, N. Iwamoto, S. Kunieda *et al.* , Nucl. Sci. Technol. 60: 1-60(2023)
[20] C. L. Lan, X. L. Yang, X. J. Li *et al.* , Nucl. Instrum. Methods Phys. Res. Sect. B 525: 18-24 (2022)
[21] C. L. Lan, Y. X. Niu, Y. T. Wei *et al*., Chin. Phys. C **47**, 094001 (2023)
[22] D. F. Mark, D. Barfod, F. M. Stuart *et al*., Geochem. Geophys. Geosyst. **10**, Q0AA02 (2009)
[23] D. He, F. M. Stuart, D. N. Barfod *et al*., Acta Geochim. **37**, 734 (2018)
[24] L. Jie, C. Wen, X. Liu *et al.* , Rock Miner. Anal. 32: 213-220 (2013)
[25] T. Shimizu, H. Sakane, S. Furuichi *et al.* , Nucl. Instrum. Methods Phys. Res. Sect. A 527(3): 543-553 (2004)
[26] Y. J. Ge, C. L. Lan, H. Y. Lv *et al*., Appl. Radait. Isotopes **200**, 110907 (2023)
[27] J. H. Luo *et al.* , Nucl. Instrum. Meth. B 359: 5-11 (2015)
[28] C. L. Lan, X. S. Xu, K. H. Fang *et al.* , Ann. Nucl. Energy 35: 2105-2108 (2008)
[29] S. Y. Sheela, H. Naik, K. M. Prasad *et al.* , Internal report no. Mu/Stastics/DAE-BRNS/2017, 10.13140/RG. 2.2. 26729.49764 (2017)
[30] M. A. Coble, M. Grove, and A. T. Calvert, Chem. Geol. 290: 75-87 (2011)
[31] A. J. Koning, S. Hilaire, and S. Goriely, Eur. Phys. J. A **59**, 131 (2023)
[32] A. J. Koning and J. P. Delaroche, Nucl. Phys. A 713: 231–310 (2003)
[33] C. Kalbach, Phys. Rev. C 33: 818–833 (1986)
[34] H. M. Hofmann, T. Mertelmeier, M. Herman, *et al*., Zeit. Phys. A **297**, 153 (1980)
[35] P. A. Moldauer, Nucl. Phys. A 344: 185–195 (1980)